A simple and high performance soliton/SPM based pulse compression/reshaping unit

NAZMI A. MOHAMMED[a,b,c], KHALIL M. ELKHAMISY[d,e], MOUSTAFA H. ALY[f,*]

[a]*Faculty of Engineering, New Cairo Academy for Science and Arts, New Cairo, Egypt*
[b]*Photonic Research Center, October 6 University, 6th of October city, Egypt*
[c]*Faculty of Engineering, the Egyptian Chinese University, Cairo, Egypt*
[d]*Electronics and Communication Engineering Department, High Institute of Engineering, El-Shorouk Academy, Cairo, Egypt*
[e]*Electronics and Communication Engineering Department, College of Engineering and Technology, Arab Academy for Science, Technology and Maritime Transport, Cairo, Egypt*
[f]*Electronics and Communication Engineering Department, College of Engineering and Technology, Arab Academy for Science, Technology and Maritime Transport, Alexandria, Egypt, Member of OSA*

In this study, a simple and high performance pulse compression/reshaping unit is designed and evaluated. This unit is soliton based for compression and self-phase modulation (SPM) based for reshaping using a dispersion compensating fiber (DCF). A remarkable 6 % compression ratio (CR) and more than 30 dB improvement in the extinction ratio (ER) are obtained. Compared to related work, a high and flexible performance is achieved.

1. Introduction

Optical time division multiplexing (OTDM) transmission technology has made a lot of progress towards much higher bit rates and much longer transmission links [1]. OTDM places lower data rate channels into unique time slots of a higher rate stream. This allows multiple channels to be placed on a single frequency where each channel can later be extracted for detection using a high-speed switch [2].

A high-quality pulse source is required to generate ultra-high bit rate serial data signals for OTDM [3]. All-optical pulse compression and reshaping are key stages for realizing a remarkable high-quality pulse source that can meet OTDM requirements [4, 5].

Several techniques were proposed to realize effective pulse compression/reshaping stages [6-9]. Among all, recently a soliton based pulse compression stage and a self-phase modulation (SPM) based pulse reshaping stage become an optimum choice [3, 10]. Using soliton based compression, a very small pulse width can be produced but with pedestal which can removed by an SPM based reshaping stage. In addition, an acceptable extinction ratio (ER) can be realized [3].

In this paper, a remarkable pulse compression and reshaping performance is realized through utilizing soliton with SPM. ER and compression/reshaping stages complexity are also addressed and evaluated.

2. Physical concept of pulse compression and reshaping

2.1. Using soliton

Soliton propagation results from a special case of nonlinear dispersion compensation in which the nonlinear chirp caused by SPM balances, and hence postpones, the temporal broadening induced by group velocity delay. Both of these phenomena limit the propagation distance that can be achieved when acting independently. If balanced at the necessary critical pulse intensity, they enable the pulse to propagate without any distortion (i.e. its shape is self-maintained) as a soliton [11].

Fig. 1 represents the general block diagram of pulse compression stage. The comb-like dispersion profile fiber (CDPF) structure is used with its alternately arranged single mode fiber (SMF) as high-dispersion segments with a dispersion shifted fiber (DSF) as low-dispersion segments in solid box with the signal intensity profile after each segment [3, 12]. The input and output signal power on this stage are presented on optical time domain visualizer (OTDV).
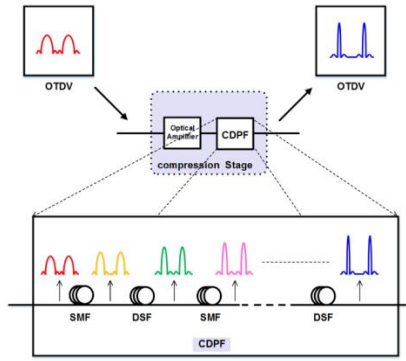
Fig. 1. Pulse compression stage and structure of CDPF

2.2. Using SPM

SPM is the main technique for realizing two essential stages of the pulse source (in pulse reshaping stage and sometimes in pulse compression stage).

A signal pulse propagates through high nonlinear fiber (HNLF) that has a small normal dispersion in order to avoid the occurrence of Raman self-frequency shifting and to achieve a symmetric spectral broadening. The amount of spectral broadening caused by SPM is affected greatly (and can be controlled) by the power level of the input signal [14, 15].

The spectral width for a Gaussian input pulse is given by [14].

$$\Delta\omega_{SPM} \sim \Delta\omega_0\, \gamma\, P_0\, L_{eff} \qquad (1)$$

where $\Delta\omega_0$ and P_0 are the initial spectral width and peak power of the input signal pulse, respectively. γ and L_{eff} are the HNLF nonlinear coefficient and effective length, respectively.

Fig. 2 shows the general block diagram of pulse reshaping stage. The blue signal OTDV is the input signal on this stage and the black signal is its output. The spectral broadening (as shown on optical spectrum analyzer (OSA)) occurs in this stage after passing the optical signal (with high intensity) through fiber with high nonlinear coefficient dispersion compensating fiber (DCF).
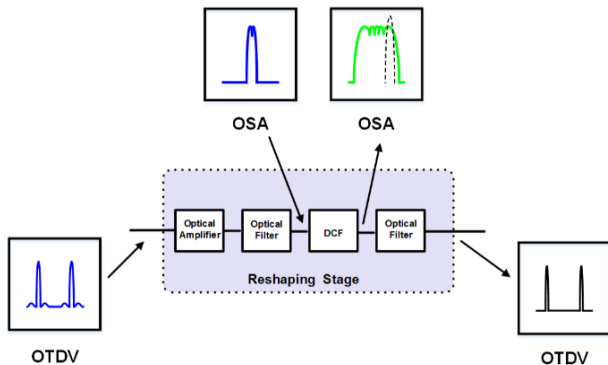
3. Simulation setup, parameters and values

The Optisystem (ver. 7) is used to design and simulate the proposed system. Fig. 3 presents a general design for an OTDM pulse source containing the key pulse compression/reshaping unit. The source design contains an initial pulse generation (IPG) stage that consists of phase modulator (PM) with (V_π= 3.5 V and modulation index= 1.2π) which inserts a cyclic frequency chirp into the input continuous wave (CW) light source beam at 1540 nm (with power of 11 dBm) including both negative and positive chirp, and a Mach-Zehnder Modulator (MZM) with (V_π=5.5 V and modulation index = π) carves the input beam into a sinusoidal form. Both PM and MZM are driven by a sinusoidal signal source.
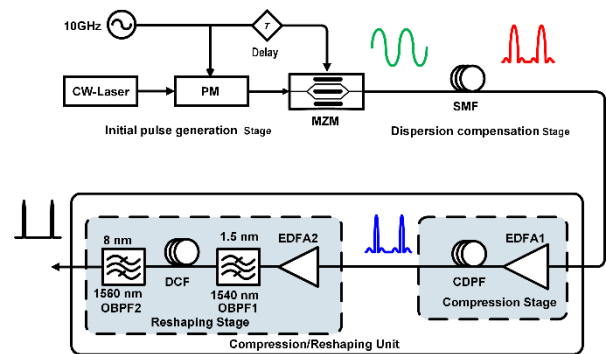

Fig. 3. Architecture of an OTDM pulse source design and pulse compression/reshaping unit

A variable electrical delay (τ), between the two modulators lets the synchronization of the phase and intensity modulations to select the sign of chirp in various parts of the beam. In this configuration, the optical pulse parts with optical intensity $I < I_{max} / 2$ is aligned with the +ve chirp, while $I > I_{max} / 2$ is aligned with the -ve chirp [3, 16]. In the Desperation Compensation (DC) stage, a 7.5 km is applied to compensate the -ve chirp [3], and the pulse train is formed. Fig. 4 represents theoretically the signal after MZM with chirp and the signal after SMF.
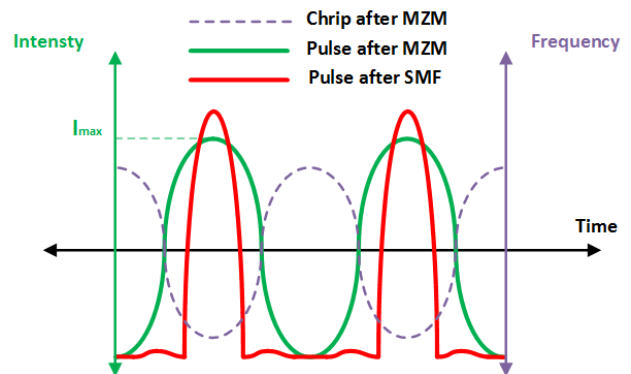

Fig. 2. Pulse reshaping stage block diagram with input and output intensity profile

Fig. 4. The signal after MZM (green) with chirp (violet dashed line) and the signal after SMF (red)

The proposed pulse compression soliton based stage consists of an erbium doped fiber amplifier (EDFA1) with 15 dB gain (the signal power value before EDFA1 is 15 dBm), and CDPF [3, 14].

In this work, and after an optimization, around 30 dBm launch into ten parts are chosen of alternately arranged 140 m SMF segments with (a GVD value of D=17ps/nm/km at 1550 nm) as high-dispersion segments with a 140 m DSF segments with negligible low dispersion have zero dispersion at 1547 nm as low-dispersion segments with total length 1.4 km. Pulses in the CDPF are influenced alternatively by nonlinear effect and group velocity dispersion (GVD) effect in space and adiabatic optical soliton transmission can be maintained and evolved in anomalous dispersion region [17]. Finally, the pulse reshaping stage that targets pedestal removing is applied [3, 10]. This stage utilizes SPM with an EDFA2 with 10 dB gain (the signal power value before EDFA2 is 30 dBm), optical power launch into the 2.5 km DCF is around 35 dBm (with dispersion of -114 ps/nm/km at 1550 nm, $\gamma \sim 2$ W^{-1}.km^{-1}). This is followed by an offset Gaussian optical band-pass filter (OBPF) with 985 GHz bandwidth at 1560 nm.

4. Results and discussion

In this work, the generated pulse width of 13 ps is entering to the pulse compression/reshaping nit (red pulse in Fig. 5). After processing through the proposed pulse compression stage, a remarkable compression is achieved with a pulse width of 1 ps (blue pulse in Fig. 5). Unfortunately, this pulse has a relatively high pulse pedestal level that makes this pulse not suitable for high quality pulse source required for OTDM applications. Therefore, the pulse reshaping stage is applied to overcome this imperfection. By considering the black pulse in Fig. 5 and after applying the offset filtering by the optimized OBPF, one can observe nearly a pedestal free pulse generation with a 0.78 ps pulse width and a compression ratio (CR) of 6%, where the CR is defined by

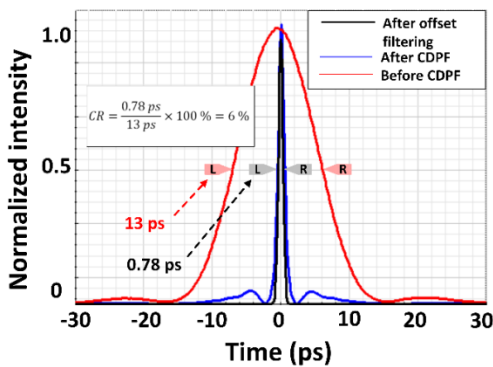$$CR = \frac{FWHM_{output\ pulse}}{FWHM_{input\ pulse}} \times 100\ \% \qquad (2)$$

Fig. 5. Signal before CDPF (red), signal after CDPF (blue) and signal after offset filtering for broadened spectrum in DCF (black)

One advantage of this scheme is its ability to improve the pulse ER simultaneously during reshaping, as shown in Fig. 6. By comparing the signal power value before and after compression/reshaping unit, the ER is improved by more than 30 dB during reshaping stage. This can be explained by: the SPM-induced chirp over pulse background is almost negligible, hence, under offset filtering, the background level can be reduced greatly and thus the pulse ER can be improved.
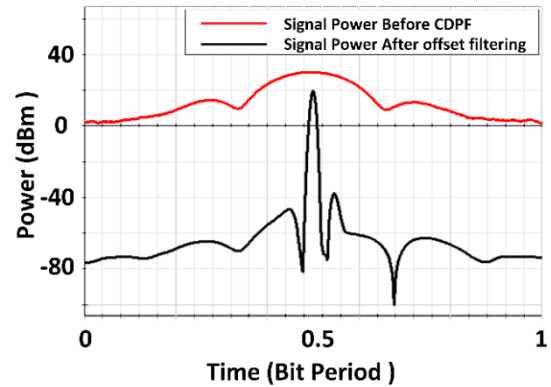
Fig. 6. Signal power before solid box (red) and after offset filtering after DCF (black)

If one needs to get a close look on the performance of the pulse reshaping stage alone one should review Fig. 7. After the pulse train (blue signal) is transmitted over the DCF, its spectrum is broadened greatly due to the SPM effect, and it has an oscillatory structure (green signal). Then, the OBPF is optimized with specifications to align its transmission center around the outermost peak of the broadened spectrum in the long wavelength direction resulting in the black signal.
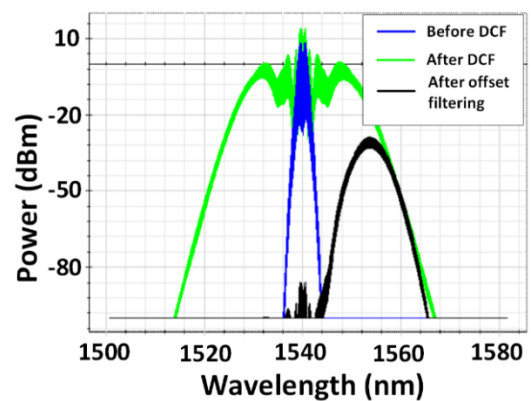
Fig. 7. Signal spectrum before DCF (blue), after DCF (green) and after offset filtering (black)

The advantages of results obtained through our work are shown when compared with related work in literature in Table 1. Specifications of input signal that enters pulse compression/reshaping stages are addressed by presenting the pulse bit rate per channel, wavelength and pulse width for input signal. Number of compression stages, compression technique and length of fiber used in

compression are the specifications of the compression stage. The previous information is re-presented for the reshaping stage. Finally, the output pulse width, CR and ER are used as performance indicators.

Table 1. Comparison with related work

Ref.	input pulse Specifications			Compression stage Specifications			Reshaping stage Specifications			Output pulse Specifications and performance indicator		
	Bitrate/ch (Gbits/s)	Wavelength (nm)	Input Pulse width (ps)	No. of Compression stages	Non-linearity effect	Length of Fiber (km)	No. of reshaping Stages	Non-linearity effect	Length of Fiber (km)	output Pulse FWHM (ps)	Compression Ratio (CR)	Extinction Ratio (ER) (dB)
[5]	10	1543.8	18	1	SPM	1 HNLF	NA	NA	NA	8.3	46.11%	30
[12]	10	1544.47	16.3	1	soliton	4.24 CDPF	1	SPM	1 HNLF	1.3	7.97%	NA
[3]	10	1543.4	12	1	soliton	4.24 CDPF	1	SPM	1 HNLF	1.4	11.66%	NA
[10]	10	1550	6	1	SPM	1.4 HNLF	1	SPM	0.8 HNLF	0.68	11.33%	NA
This article	10	1540	13	1	soliton	1.4 CDPF	1	SPM	2.5 DCF	0.78	6%	45

To explore the complexity of pulse compression/reshaping unit, which is one of this work interest, a brief comparison is presented. For pulse compression stage, and comparing with related literates that utilize same compression technique (i.e., CDPF), one can observe that this work uses a much lower fiber length (1.4 km). A similar observation is valid for the pulse reshaping stage noting that identical reshaping stage technique are common in Table 1, in contrast with pulse compression stage that has two compression techniques.

5. Conclusion

This work presents a simple design for a soliton based pulse compression stage and an SPM based pulse reshaping stage using dispersion compensating fiber (DCF). A remarkable performance is achieved having a low pulse CR (6 %) and a high ER (is improved by more than 30 dB). This design is a suitable candidate for realizing a remarkable pulse source for OTDM applications.

References

[1] Hans-Georg Weber, Reinhold Ludwig, Sebastian Ferber, Carsten Schmidt- Langhorst, Marcel Kroh,Vincent Marembert, Christof Boerner, Colja Schubert, J. Lightw. Technol. **24**, 4616 (2006).

[2] Keith G. Petrillo, Mark A. Foster, Optics Express **21**, 508 (2013).

[3] Jianhua Chen, Caiyun Lou, Li Huo, Dan Lu, Appl. Opt. **50**, 1979 (2011).

[4] K. K. Chow, C. Shu, Chinlon Lin, Quantum Electronics and Laser Science Conference, Baltimore, Maryland United States 839 (2005).

[5] Yanfu Yang, Caiyun Lou, Hongbo Zhou, Jiajun Wang, Yizhi Gao, Appl. Opt. **45**, 7524 (2006).

[6] G. P. Agrawal, Application of Nonlinear Fiber Optics, Academic Press 2001.

[7] K. Suzuki, K. Iwatsuki, S. Nishi, M. Saruwatari, K. Sato, K. Wakita, Electron. Lett. **29**, 1713 (1993).

[8] K. Igarashi, J. Hiroishi, T. Yagi, S. Namiki, Electron. Lett. **41**, 688 (2005).

[9] L. Huo, C. Lou, Y. Gao, Chinese Phys. Lett. **22**, 353 (2005).

[10] Hao Hu, Hans Christian Hansen Mulvad, Christophe Peucheret, Michael Galili, Anders Clausen, Palle Jeppesen, Leif Katsuo Oxenløwe, Optics Express **19**, B343 (2011).

[11] John M. Senior, Optical Fiber Communications Principles and Practice, Prentice Hall, 2009.

[12] Yanfu Yang, Caiyun Lou, Yizhi Gao, Optical Engineering **45**, 055004-1 (2007).

[13] Nazmi A. Mohammed, Mahmoud M. Ragab, Moustafa H. Aly, European Journal of Scientific Research **74**, 176 (2012).

[14] Y. Okawachi, R. Salem, A. L. Gaeta, J. Lightw. Technol. **25**, 3710 (2007).

[15] Nazmi A. Mohammed, Mahmoud M. Ragab, Moustafa H. Aly, International Journal of Engineering Science and Technology **4**, 324 (2012).

[16] Q. Wang, C. Lou, L. Huo, D. Lu, H. F. Li, Communication and Photonics Conference, Shanghai, China Proc. of (SPIE-OSA-IEEE) 8309201 (2011).

[17] M. Han, C.-Y. Lou, Y.We, G.-Q. Chang, Y.-Z. Gao, Y.-H. Li, Chin. Phys. Lett. **17**, 806 (2000).

*Corresponding author: mosaly@aast.edu